Journal of Theoretical and Applied Physics (2020) 14:359–365
https://doi.org/10.1007/s40094-020-00392-3

RESEARCH

Terahertz emission during laser-plasma interaction: effect of electron temperature and collisions

Hitendra K. Malik[1] · **Divya Singh**[2]

Received: 21 July 2020 / Accepted: 23 August 2020 / Published online: 5 September 2020

Abstract

The electron-neutral collisions in the plasma become crucial with regard to the generation of THz radiation when thermal motion of the electrons is considerable. If we look at the mechanism of THz emission, this is only the movement/oscillations of the electrons which is responsible for the excitation of nonlinear current that generated the THz radiation. The present work aims to disclose the role of thermal motion of the plasma electrons to the resonance condition and the THz emission when two co-propagating super-Gaussian laser beams beat in the plasma. The dynamics of the plasma electrons and subsequent generation of nonlinear current are discussed in greater detail for the emission of THz radiation.

Keywords Laser-plasma interaction · Ponderomotive force · Terahertz radiation · Electron temperature · Super-Gaussian laser · Efficiency

Introduction

Several applications such as characterization of materials, imaging, communication, medical diagnostics make use of THz radiations for their better efficiency. The frequency of these radiations lies between 100 GHz and 10 THz. These radiations can be achieved by various mechanisms which include Cherenkov wakes [1–3] and inverse Compton scattering based on X-ray radiation [4]; even soft X-rays have been found to emit from TIN plasmas [5]. The interaction of laser pulses with magnetized plasma has led to the emission of THz radiation [6–8]. Some instabilities can be responsible for the emission of such radiation [9]. Laser beating is one of the mechanisms of producing the THz radiation [10]. Some researchers have also established a relationship between the signals corresponding to the THz radiation and X-rays [11]. Magnetic field has been found to enhance the intensity of the emitted THz radiation in laser-plasma interaction [12]. The tunnel ionized plasma can also radiate when a femtosecond laser pulse is launched to this and where dipole oscillations take place due to the residual momentum imparted by the lasers to the plasma electrons [13]. Extremely powerful THz radiations have also been achieved by interaction of chirped [14] and few cycle laser pulses [15] with plasmas.

The above literature proves that the spatial profile of the laser pulses is very important for achieving the THz radiation of specific characteristics during the interaction of laser beams with plasmas. The temporal profile of the lasers has also played an important role in other mechanisms [16, 17]. For laser-plasma interaction, Ostermayr et al. [18] and Devi and Malik [19] have employed super-Gaussian pulses of laser beam for achieving the particle acceleration and to get the self-focusing effect in plasmas, respectively. In almost all the work, people have neglected thermal motion of the plasma electrons during laser-plasma interaction, when talked about the THz radiation generation in a collisional plasma. However, this is vital to understand the impact of finite temperature of the electrons for the emission of THz radiation in a collisional plasma, as these two effects are correlated and should be analyzed together. Hence, the present work is aimed at examining the combined effect of electron-neutral collisions and electron temperature on the emitted THz radiation when two co-propagating super-Gaussian laser beams beat in the plasma.

✉ Hitendra K. Malik
hkmalik@hotmail.com

[1] Plasma Waves and Particle Acceleration (PWAPA) Laboratory, Department of Physics, Indian Institute of Technology, Delhi, New Delhi 110 016, India

[2] Rajdhani College, Delhi University, Delhi, New Delhi, India

Dynamics of plasma electrons

We consider a propagation of two linearly polarized lasers of frequencies ω_1 and ω_2, and wave numbers k_1 and k_2, respectively, in the z direction of preformed plasma of density N_0. The field of the lasers is assumed as

$$\vec{E}_j = E_0 \exp\left[i\left(k_j z - \omega_j t\right)\right]\hat{y}, \tag{1}$$

where E_0 has super-Gaussian (sG) field profile, and $j=1$ and 2. The motion of plasma electrons is described by the momentum equation, whereas plasma ions remain unaffected being heavier than the electrons; hence, these are considered to be immobile. Consistently, the plasma is taken to be weakly ionized where the electron-neutral collisions (frequency $\nu_{en}=\nu$) are present. T_0 is taken to be the equilibrium temperature of the plasma electrons. For the matching of wave number of ponderomotive force and the nonlinear current, we shall require space-periodically modulated density $N=N_0+N_\alpha e^{i\alpha z}$ together with N_α as the amplitude and α as the wave number of the density ripples along the direction of propagation of the lasers. On passage of the lasers along the z-axis, the plasma electrons are under the action of lasers fields (polarized in y-direction). The force acting on them is expressed through the equation of motion, i.e.,

$$m\frac{\partial \vec{v}}{\partial t} = -e\vec{E} - m\nu\vec{v}, \tag{2}$$

in the presence of collisions (frequency ν).

Ponderomotive force by super-Gaussian laser profile

The field of the super-Gaussian lasers is assumed as

$$E_0 = E_{0L}\exp\left[-\left(\frac{y}{b_w}\right)^p\right]. \tag{3}$$

Here p represents the index of the laser beams and $p>2$ (even numbers) represents the case of super-Gaussian lasers, whereas $p=2$ would represent the Gaussian laser only. The super-Gaussian beams have highest field/intensity (peak) for larger region on the axis, whereas the field/intensity of the Gaussian beams is within a smaller region. Because of this, the gradient in the intensity of the super-Gaussian beams and hence the ponderomotive force is larger than the Gaussian beams. The ponderomotive force is realized at the frequency $\omega=\omega_1-\omega_2$ and wave number $k=k_1-k_2$, and the oscillatory velocity of the electrons is obtained from Eq. (2) as

$$\vec{v}_j = \frac{e\vec{E}_j}{m(i\omega_j - \nu)}. \tag{4}$$

The corresponding ponderomotive potential is calculated from the expression $\varphi_p = -\frac{m}{2e}(\vec{v}_1\cdot\vec{v}_2\,*)$. Hence, the ponderomotive force is obtained as

$$\vec{F}_p^{NL} = \frac{e^2E_{0L}^2}{2m(i\omega_1-\nu)(i\omega_2+\nu)}\exp\left[-2\left(\frac{y}{b_w}\right)^p\right]\left[\frac{2p}{b_w}\left(\frac{y}{b_w}\right)^{p-1}\hat{y} - ik\hat{z}\right]\exp\left[i(kz-\omega t)\right]. \tag{5}$$

Generation of plasma currents

The motion of plasma electrons is modified due to the ponderomotive force and the pressure gradient force which appears due to the finite temperature of the electrons. Let us find out nonlinear velocity of these electrons $\vec{v}^{NL}$ by using the following equation of motion and equation of continuity

$$mN_0\frac{\partial\vec{v}^{NL}}{\partial t} = N_0\vec{F}_P^{NL} - mN_0\nu\vec{v}^{NL} - k_BT_0\vec{\nabla}N^{NL}, \tag{6}$$

$$\frac{\partial N^{NL}}{\partial t} + N_0(\vec{\nabla}\cdot\vec{v}^{NL}) = 0, \tag{7}$$

Here k_B represents the Boltzmann constant and its value in CGS units is $k_B=1.38\times10^{-16}$ cm^{2}g/s^{2}K. The above equations yield

$$\vec{v}^{NL} = \frac{\omega\vec{F}_p^{NL}}{\left[m\nu\omega - i\left(m\omega^2 - k^2k_BT_0\right)\right]}. \tag{8}$$

Based on this we evaluate the nonlinear current density developed in the plasma. This is given by

$$N^{NL} = \frac{N_0\vec{\nabla}\cdot\vec{F}_p^{NL}}{m\left[\left(\omega^2 - k^2v_{th}^2\right) + i\nu\omega\right]}. \tag{9}$$

The nonlinear density may also be expressed in terms of the electrical susceptibility of the plasma as $N^{NL} = -\frac{\chi_eN_0\vec{\nabla}\cdot\vec{F}_p^{NL}}{m\omega_p^2}$, where $\chi_e = -\frac{\omega_p^2}{\left[(\omega^2-k^2v_{th}^2)+i\nu\omega\right]}$, and $v_{th}^2 = \frac{k_BT_e}{m}$. This is clear that the electrical susceptibility of the plasma has been modified due to the finite temperature of the plasma. For the cold plasma, where $T_e=0$ ($v_{th}=0$), however, this expression takes the form of susceptibility derived by other researchers in unmagnetized cold plasma [20] and magnetized cold plasma with the neglect of external magnetic field [12].

The linear density perturbations caused by N^{NL} are given as below

$$N^L = -\frac{\chi_eN_0e\vec{\nabla}\cdot\vec{\nabla}\varphi}{m\omega_p^2}. \tag{10}$$

Clearly these perturbations are also affected by the finite temperature of plasma electrons. Now we calculate the force $\vec{F}^L$, which takes the contribution of N^{NL} and N^L. This is obtained as

$$\vec{F}^L = e\vec{\nabla}\varphi = \frac{\omega_p^2 \vec{F}_p^{NL}}{i\omega\left(1+\chi_e\right)(\nu - i\omega)}. \tag{11}$$

The resultant transverse nonlinear electron velocity under the combined action of forces $\vec{F}^L$ and $\vec{F}_p^{NL}$ is obtained as

$$\vec{v}_y' = \frac{\omega^2(\omega+i\nu)^2 - k^2 v_{th}^2[\omega(\omega+i\nu)+\omega_p^2]}{m\omega(\omega+i\nu)^2[\omega(\omega+i\nu)-(\omega_p^2+k^2v_{th}^2)]} i\vec{F}_{py}^{NL}. \tag{12}$$

Based on $\vec{J}^{NL} = -\frac{1}{2}N'e\vec{v}_y'$, where $N' = N_\alpha e^{i\alpha z}$ yields the following nonlinear oscillatory current density

$$J_y^{NL} = -\frac{1}{4}i\frac{N_\alpha}{m^2\omega(\omega+i\nu)^2}\frac{e^3E_{0L}^2}{(i\omega_1-\nu)(i\omega_2+\nu)} \frac{[\omega^2(\omega+i\nu)^2 - k^2v_{th}^2\{\omega(\omega+i\nu)+\omega_p^2\}]}{[\omega(\omega+i\nu)-(\omega_p^2+k^2v_{th}^2)]} \times \frac{2p}{b_w}\left(\frac{y}{b_w}\right)^{p-1}\exp\left[-2\left(\frac{y}{b_w}\right)^p\right]e^{i\{(k+\alpha)z-\omega t\}}. \tag{13}$$

This current is mainly responsible for the resonant generation of THz radiation provided phase matching condition is satisfied. Here it can be seen that $\vec{J}^{NL}$ is modified due to the term v_{th}^2 or the finite temperature of the electrons. In order to check the authenticity of the calculations, we discuss the limiting case for the cold plasma ($v_{th} = 0 = T_e$) which was discussed earlier. This can be seen that $\vec{J}^{NL}$ takes the same form as obtained by other investigators for $T_e = 0$. For example, it reduces to the expression obtained in Ref. [20] when $T_e = 0$. On the other hand, this expression is the same when one neglects the cyclotron motion of the electrons in the investigation carried out in Ref. [12].

Discussion on modified resonance and phase matching condition

Equation (13) shows that the nonlinear current $\vec{J}^{NL}$ oscillates at the frequency ω, but its wave number is $k+\alpha$. This is clear that the matching of wave number has been done with the application of periodicity of the density ripples. Further, in order to obtain the amplitude of THz radiation, we have made use of the following condition in Eq. (16), later

$$\left(\frac{\alpha c}{\omega_p}\right) = \frac{\omega}{\omega_p}\left[\left(1 - \frac{\omega_p^2}{\{\omega(\omega+i\nu)-k^2v_{th}^2\}}\right)^{1/2} - 1\right]. \tag{14}$$

The real part of above condition is represented as

$$\mathrm{Re}\left(\frac{\alpha c}{\omega_p}\right) = \frac{\omega}{\omega_p}\left[\left(1 - \frac{\omega_p^2(\omega^2 - k^2v_{th}^2)}{\{(\omega^2-k^2v_{th}^2)^2+\omega^2\nu^2\}}\right)^{1/2} - 1\right]. \tag{15}$$

This is the required condition for the resonant excitation of THz radiation. Clearly, the resonance condition has been modified due to the finite temperature T_e of the electrons via the term v_{th}^2 in Eq. (15). If we look at the resonance condition, we find that the condition $\omega = \omega_p$ obtained in the collision-less plasma is departed due to the electron-neutral collisions and thermal motion of plasma electrons in the present case, and hence, the resonance condition modifies. The modified resonance condition in the present case of finite temperature plasma reads $\omega = \sqrt{\omega_p^2 + \nu^2 + k_B^2 v_{th}^2}$.

Figure 1 shows the variation of normalized ripple wave number $\alpha c/\omega_p$ with the temperature T_e. This is evident that α increases with the increase of temperature. The nature of variation, i.e., the increase of wave number with the temperature, remains the same for different values of collision frequency ν. It means the density ripples should be constructed at smaller distances in the case of finite temperature plasma for the resonant excitation of the THz radiation. However, the opposite behavior of α with beat wave frequency ω (Fig. 2) and collision frequency ν (Fig. 3) is observed. This variation suggests that the ripples should be constructed at larger distances if the collision frequency or the beat wave frequency is enhanced in the plasma.

A comparative study of Figs. 1, 2 and 3 reveals that the impact of collisions is much significant on the ripples wave number in comparison with the effect of thermal motion of the

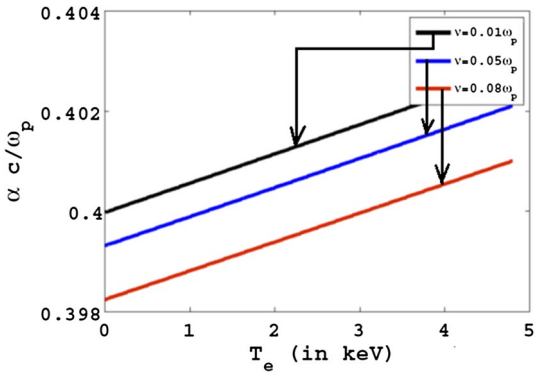

Fig. 1 Variation of normalized ripple wave number with electron temperature for various collision rates of plasma electrons with neutrals when $\omega = 2.4\times10^{14}$ rad/s and $\omega_p = 2.0\times10^{13}$ rad/s

electrons. Keeping in mind the variation of $\alpha c/\omega_p$ with T_e, ν and ω, one can optimize the separation of density ripples in the plasma for the resonant excitation of the THz radiation. The optimization can be done based on Eq. (15). The separation and amplitude of the density ripples in plasma can be achieved experimentally. For example, the use of laser machining with a liquid–crystal spatial light modulator can create the pattern mask [21]. Periodic tunnel ionization and strong ripples in plasma can be achieved by focusing of two counter propagating laser beams through axicon lens [22]. There are other techniques also which can create the periodic density ripples [23–25] in plasma and where the periodicity and size can also be controlled by using standing waves created by microwave radiation [25].

Calculation of field of THz radiation

We make use of the following wave equation for obtaining the field of the THz radiation (say E_{THz})

$$-\nabla^2\vec{E}_{\mathrm{THz}} + \vec{\nabla}\left(\vec{\nabla}\cdot\vec{E}_{\mathrm{THz}}\right) = -\frac{4\pi i\omega}{c^2}\vec{J}^{NL} + \frac{\omega^2}{c^2}\varepsilon\vec{E}_{\mathrm{THz}}. \quad (16)$$

However, we shall use the modified expression of ε due to finite temperature T_e, given as

$$\varepsilon = 1 + \chi_e = 1 - \frac{\omega_p^2}{[(\omega^2 - k^2v_{th}^2) + i\nu\omega]}, \quad (17)$$

The use of Eqs. (15) and (17) in Eq. (16) gives rise to the following expression for E_{THz}

$$E_{\mathrm{THz}} = -\frac{\omega_p^2 eE_{0L}^2}{4m\omega^2}\frac{N_\alpha}{N_0}\frac{[\omega(\omega+i\nu)-k^2v_{th}^2][\omega^2(\omega+i\nu)^2-k^2v_{th}^2\{\omega(\omega+i\nu)+\omega_p^2\}]}{(\omega+i\nu)^2(i\omega_1-\nu)(i\omega_2+\nu)[\omega(\omega+i\nu)-(\omega_p^2+k^2v_{th}^2)]} \times \frac{2p}{b_w}\left(\frac{y}{b_w}\right)^{p-1}\exp\left[-2\left(\frac{y}{b_w}\right)^p\right]e^{i\{(k+\alpha)z-\omega t\}}. \quad (18)$$

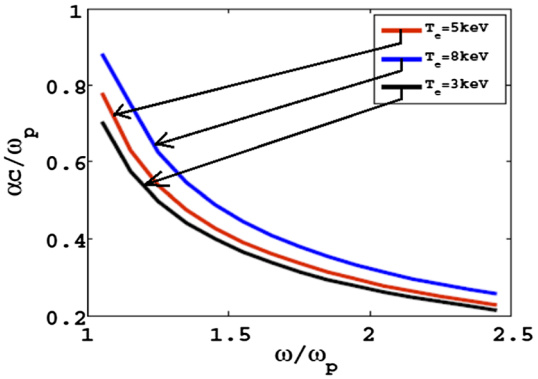

Fig. 2 Variation of normalized ripple wave number with normalized resonant frequency for different electron temperature when $\omega_p = 2.0\times10^{13}$ rad/s and $\nu = 0.01\omega_p$

The real part of the above relation shall be the magnitude of the THz radiation field E_{0THz}. The normalized form of E_{0THz} is obtained as

$$\frac{E_{0THz}}{E_{0L}} = -\frac{\omega_p^2 eE_{0L}}{4m}\frac{N_\alpha}{N_0}\frac{2p}{b_w}\left(\frac{y}{b_w}\right)^{p-1}H_R\exp\left[-2\left(\frac{y}{b_w}\right)^p\right] \quad (19)$$

where H_R reads

$$H_R = \mathrm{Re}\left\{\frac{[\omega(\omega+i\nu)-k^2v_{th}^2][\omega^2(\omega+i\nu)^2-k^2v_{th}^2\{\omega(\omega+i\nu)+\omega_p^2\}]}{\omega^2(\omega+i\nu)^2(i\omega_1-\nu)(i\omega_2+\nu)[\omega(\omega+i\nu)-(\omega_p^2+k^2v_{th}^2)]}\right\}. \quad (20)$$

This is clear that the amplitude of E_{0THz} is affected by the finite temperature T_e of the electrons due to the appearance of the term v_{th}.

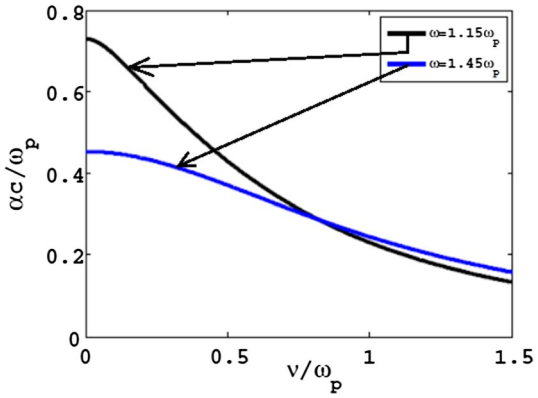

Fig. 3 Variation of normalized ripple wave number with normalized collision frequency for various plasma resonant frequencies when $\omega_p = 2.0\times10^{13}$ rad/s and $T_e = 3$ keV

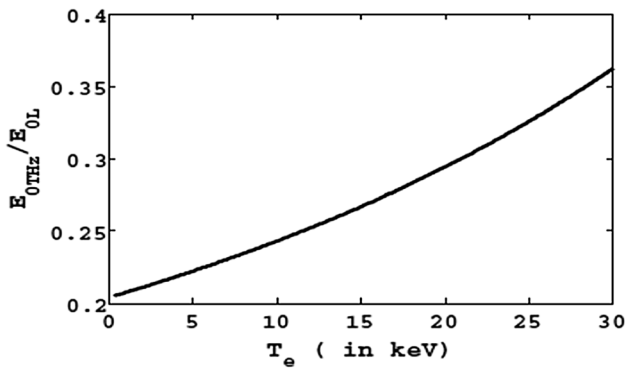

Fig. 4 Variation of normalized magnitude of emitted THz radiation field with electron temperature when $\omega = 2.4\times10^{14}$ rad/s, $\omega_p = 2.0\times10^{13}$ rad/s, $\nu = 0$, $E_0 = 5.0\times10^8$ V/cm, $y = 0.8b_w$, $p = 6$, and $N_\alpha/N_0 = 0.4$

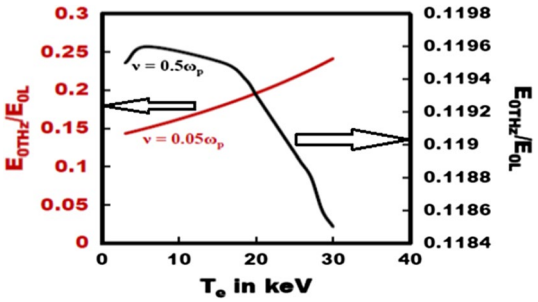

Fig. 5 Variation of normalized magnitude of emitted THz radiation with electron temperature in the presence of low ($\nu = 0.05\omega_p$) or high ($\nu = 0.5\omega_p$) collisions, when $b_w = 0.01$ cm, $\omega = 2.4 \times 10^{14}$ rad/s, $\omega_p = 2.0 \times 10^{13}$ rad/s, $E_0 = 5.0 \times 10^8$ V/cm, $y = 0.8b_w$ and $p = 6$

Effect of electron-neutral collisions on THz field

Figure 4 shows the variation of normalized THz amplitude with electron temperature in collision-less plasma ($\nu = 0$), depicting the enhancement of THz field with temperature. Figure 5 shows the variation of normalized THz field amplitude with electron temperature for two values of collision frequency as $\nu = 0.05\ \omega_p$ and $\nu = 0.5\ \omega_p$. Figure 6 depicts the situation of collision frequency $\nu = 0.45\ \omega_p$ and $\nu = 0.6\ \omega_p$.

It is evident from Figs. 4 and 5 that the thermal motion of the electrons supports the THz emission as the amplitude of THz field is enhanced with increasing T_e. This is true for the collision-less plasma or the plasma where $\nu \ll \omega_p$. However, for the case of larger collision frequency, negative impact of electron temperature T_e is realized and we get diffused THz emission for the higher electron temperature. This reveals that one should include the electron temperature when the electron-neutral collisions sustain in the plasmas. When we focus on Fig. 6, we realize that there is an optimum value of collision frequency below which the electron temperature helps achieving the stronger THz emission. On the other hand, if the collision frequency is larger than this optimum value of ν, the electron temperature reduces the emission of THz radiation.

Since the present mechanism talks about the resonant excitation of THz emission via the nonlinear current density $\vec{J}^{NL}$, the reason for an optimum combination of the collision frequency ν and electron temperature T_e for the maximum THz amplitude may be attributed to the nonlinearity of the plasma. This is plausible that the plasma becomes highly nonlinear at this optimum combination of ν and T_e. It means the collisions and thermal motions of electrons play a vital role in setting up the nonlinearity in the plasma via the modified electrical susceptibility or the dielectric constant of the plasma. Under this situation, an enhanced (maximum) current is excited that leads to the maximum radiation through the oscillations of plasma electrons.

Effect of electron temperature on THz field

Through Fig. 7 we uncover the role of electron temperature T_e on the resonant excitation of the THz radiation. This is evident from this figure that there is a peak of THz amplitude at a particular value of ω/ω_p, which is not at $\omega/\omega_p = 1$, i.e., at $\omega = \omega_p$.

In the absence of collisions, the resonance is achieved when beat wave frequency matches with the plasma frequency ($\omega = \omega_p$), leading to maximum transfer of laser energy to THz radiation through nonlinear current. However, collisions bring a slight departure in the resonance condition, i.e., resonance occurs at $\omega \approx \sqrt{\omega_p^2 + \nu^2}$. On the other hand, in the present case of collisional plasma where electron thermal motion is also considerable, the resonance condition has been drastically modified, being around $\omega \approx \sqrt{\omega_p^2 + \nu^2 + k_B^2 v_{th}^2}$. Because of this we realize

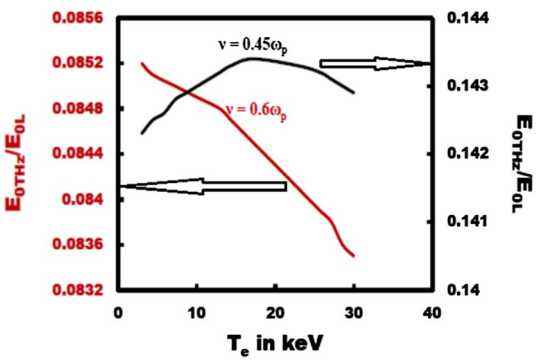

Fig. 6 Variation of normalized magnitude of emitted THz radiation with electron temperature in the presence of collisions with SG laser of beam width $b_w = 0.01$ cm when $\omega = 2.4 \times 10^{14}$ rad/s, $\omega_p = 2.0 \times 10^{13}$ rad/s, $E_0 = 5.0 \times 10^8$ V/cm, $y = 0.8b_w$ and $p = 6$

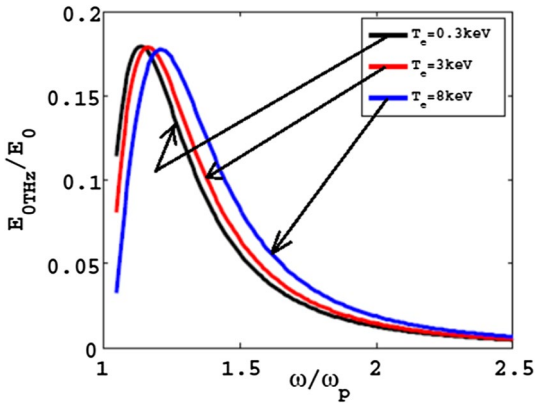

Fig. 7 Effect of resonance frequency on normalized magnitude of emitted THz radiation at different electron temperatures when $\omega_p = 2.0 \times 10^{13}$ rad/s, $E_0 = 5.0 \times 10^8$ V/cm, $y = 0.8b_w$ $p = 6$ and $\nu = 0.05\ \omega_p$

a shift in the peak of THz amplitude in Fig. 7. The peak refers to the resonance where maximum energy and momentum from lasers to plasma electrons are transferred for the generation of nonlinear current and then the THz radiation. Hence, the role of electron temperature is to shift the frequency and amplitude of the emitted THz radiation.

Efficiency of THz radiation mechanism

We employ the similar approach, as used in Refs. [10, 12, 20], for obtaining the efficiency of THz radiation. Hence, the efficiency (say η) is obtained using the following formula

$$\eta = \frac{\langle W_{\mathrm{THz}E}\rangle}{\langle W_{LE}\rangle}. \tag{21}$$

For the present case of super-Gaussian lasers and collisional plasma, we obtain

$$\langle W_{LE}\rangle = \frac{1}{8\pi}\frac{b_w E_{0L}^2}{2^{\frac{1}{p}-1}}\frac{\Gamma 1/p}{p}, \tag{22}$$

and

$$\langle W_{\mathrm{THz}E}\rangle = \frac{1}{8\pi}\frac{2b_w E_{0THz}^2}{4p}\frac{\Gamma(2-1/p)}{4^{1-\frac{1}{p}}}. \tag{23}$$

where Γ is the Gamma function. Finally, the efficiency η reads

$$\eta = \frac{2^{\left(\frac{3-4p}{p}\right)}\Gamma(2-1/p)}{\Gamma(1/p)}\left[\frac{\omega_p^2}{4m}\frac{N_\alpha}{N_0}\frac{2peE_{0L}}{b_w}H_R\right]^2, \tag{24}$$

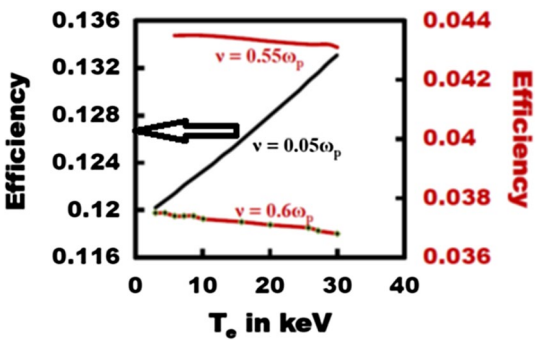

Fig. 8 Variation of efficiency of the mechanism of emitted THz radiation with electron temperature in the presence of collisions, when $b_w = 0.01$ cm, $\omega = 2.4\times10^{14}$ rad/s, $\omega_p = 2.0\times10^{13}$ rad/s, $E_0 = 5.0\times10^8$ V/cm, $y = 0.8b_w$ and $p = 6$

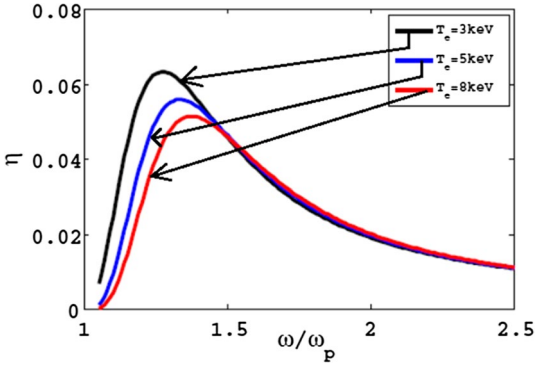

Fig. 9 Variation of efficiency of the mechanism of emitted THz radiation with normalized resonance frequency for different electron temperatures, when $\omega_p = 2.0\times10^{13}$ rad/s, $\nu = 0.05\ \omega_p$, $E_0 = 5.0\times10^8$ V/cm, $p = 6$ and $y = 0.8b_w$

where all the symbols have already been defined and have their usual meanings.

Figure 8 depicts the variation of the efficiency of the mechanism of THz radiation generation with electrons temperature for different values of collisional rates. Consistent to the observations of THz field amplitude, the efficiency increases straight with temperature in the presence of low collisions $\nu = 0.05\ \omega_p$, whereas the efficiency decays for the larger collisions in the plasma ($\nu = 0.55\omega_p$ and $0.6\omega_p$).

On the other hand, the efficiency attains a maximum value at a particular value of beating frequency (Fig. 9). However, lower efficiency is attained for the frequency larger or lower than this critical frequency. This critical frequency is actually the resonance frequency where the maximum transfer of momentum and energy takes place. Interestingly this peak or the resonance frequency is shifted when the electron temperature is changed.

Conclusions

It is concluded that the resonance condition for maximum amplitude of emitted THz radiation is altered in the presence of thermal motion of the electrons in collisional plasma, but the frequency of emitted radiation can be tuned by changing electron temperature T_e owing to the thermal effects involved in the process. The amplitude of the emitted THz radiation varies differently with collisional effects. In the presence of low collision frequency $\nu < 0.5\omega_p$, thermal motions support the THz emission. However, in the presence of high-frequency collision $\nu > 0.5\omega_p$, the THz amplitude is found to decrease with the increased electron temperature.

References

1. Jung, C.: International seminar on advanced accelerator and radiation physics. Synchrotron Radiat. News **29**, 11–13 (2016)
2. Li, X.F., Yu, Q., Gu, Y.J., Qu, J.F., Ma, Y.Y., Kong, Q., Kawata, S.: Calculating the radiation characteristics of accelerated electrons in laser-plasma interactions. Phys. Plasmas **23**(3), 033113 (2016)
3. Starodubtsev, M., Krafft, C., Lundin, B., Thévenet, P.: Resonant Cherenkov emission of whistlers by a modulated electron beam. Phys. Plasmas **6**(7), 2862–2869 (1999)
4. Lemos, N., Martins, J.L., Tsung, F.S., Shaw, J.L., Marsh, K.A., Albert, F., Joshi, C.: Self-modulated laser wakefield accelerators as x-ray sources. Plasma Phys. Control. Fusion **58**(3), 034018 (2016)
5. Demir, P., Kacar, E., Akman, E., Bilikmen, S.K., Demir, A.: Theoretical and experimental investigation of soft x-rays emitted from TIN plasmas for lithographic application. In *Ultrafast X-Ray Sources and Detectors* (Vol. 6703, p. 67030B). International Society for Optics and Photonics (2007)
6. Dorranian, D., Ghoranneviss, M., Starodubtsev, M., Ito, H., Yugami, N., Nishida, Y.: Generation of short pulse radiation from magnetized wake in gas-jet plasma and laser interaction. Phys. Lett. A **331**(1–2), 77–83 (2004)
7. Dorranian, D., Ghoranneviss, M., Starodubtsev, M., Yugami, N., Nishida, Y.: Microwave emission from TW-100 fs laser irradiation of gas jet. Laser Part. Beams **23**(4), 583–596 (2004)
8. Manouchehrizadeh, M., Dorranian, D.: Effect of obliqueness of external magnetic field on the characteristics of magnetized plasma wakefield. J. Theor. Appl. Phys. **7**(1), 43 (2013)
9. Starodubtsev, M., Kamal-Al-Hassan, M., Ito, H., Yugami, N., Nishida, Y.: Low-frequency sheath instability stimulated by an energetic ion component. Phys. Plasmas **13**(1), 012103 (2006)
10. Malik, A.K., Malik, H.K., Nishida, Y.: Terahertz radiation generation by beating of two spatial-Gaussian lasers. Phys. Lett. A **375**(8), 1191–1194 (2011)
11. Mun, J., Park, S., Yea, K.: Relationship between Terahertz and X-ray signals generated from laser-induced plasma on gas targets. J. Korean Phys. Soc. **56**(11), 275–278 (2010)
12. Singh, D., Malik, H.K.: Enhancement of terahertz emission in magnetized collisional plasma. Plasma Sources Sci. Technol. **24**(4), 045001 (2015)
13. Malik, A.K., Malik, H.K., Kawata, S.: Investigations on terahertz radiation generated by two superposed femtosecond laser pulses. J. Appl. Phys. **107**(11), 113105 (2010)
14. Wang, W.M., Sheng, Z.M., Wu, H.C., Chen, M., Li, C., Zhang, J., Mima, K.: Strong terahertz pulse generation by chirped laser pulses in tenuous gases. Opt. Express **16**(21), 16999–17006 (2008)
15. Wang, W.M., Kawata, S., Sheng, Z.M., Li, Y.T., Zhang, J.: Towards gigawatt terahertz emission by few-cycle laser pulses. Phys. Plasmas **18**(7), 073108 (2011)
16. Malik, L., Escarguel, A.: Role of the temporal profile of femtosecond lasers of two different colours in holography. EPL (Europhys. Lett.) **124**(6), 64002 (2019)
17. Malik, L.: Dark hollow lasers may be better candidates for holography. Opt. Laser Technol. **132**, 106485 (2020)
18. Ostermayr, T., Petrovics, S., Iqbal, K., Klier, C., Ruhl, H., Nakajima, K., Li, R.: Laser plasma accelerator driven by a super-Gaussian pulse. J. Plasma Phys. **78**(4), 447–453 (2012)
19. Devi, L., Malik, H.K.: Resonant third harmonic generation of super-Gaussian laser beam in a rippled density plasma. J. Theor. Appl. Phys. **12**(4), 265–270 (2018)
20. Singh, D., Malik, H.K.: Terahertz generation by mixing of two super-Gaussian laser beams in collisional plasma. Phys. Plasmas **21**(8), 083105 (2014)
21. Hung, T.S., Ho, Y.C., Chang, Y.L., Wong, S.J., Chu, H.H., Lin, J.Y., Chen, S.Y.: Programmably structured plasma waveguide for development of table-top photon and particle sources. Phys. Plasmas **19**(6), 063109 (2012)
22. Sheng, Z.M., Zhang, J., Umstadter, D.: Plasma density gratings induced by intersecting laser pulses in underdense plasmas. Appl. Phys. B **77**(6–7), 673–680 (2003)
23. Kim, K.Y., Taylor, A.J., Glownia, J.H., Rodriguez, G.: Coherent control of terahertz supercontinuum generation in ultrafast laser–gas interactions. Nat. Photon. **2**(10), 605–609 (2008)
24. Kuo, C.C., Pai, C.H., Lin, M.W., Lee, K.H., Lin, J.Y., Wang, J., Chen, S.Y.: Enhancement of relativistic harmonic generation by an optically preformed periodic plasma waveguide. Phys. Rev. Lett. **98**(3), 033901 (2007)
25. Malik, H.K.: Density bunch formation by microwave in a plasma-filled cylindrical waveguide. EPL (Europhys. Lett.) **106**(5), 55002 (2014)